Radiative lifetime measurement of the 3^1S, 3^1D, 4^1D, 4^1F, and 5^1F excited states of helium

George A. Khayrallah* and S. J. Smith†
Joint Institute for Laboratory Astrophysics, University of Colorado and National Bureau of Standards, Boulder, Colorado 80309
(Received 13 February 1978)

The lifetimes of the 3^1S, 3^1D, 4^1D, 4^1F, and 5^1F states of He have been determined experimentally to be 54.5 ± 0.8, 16.7 ± 0.8, 36.4 ± 1.2, 67 ± 10, and 142 ± 20 nesc, respectively. The measurements were made at several incident electron energies using a pulsed-electron time-delayed-coincidence technique.

I. INTRODUCTION

Helium, being the next simplest atom after hydrogen, is accessible to relatively direct calculation of its properties, and has attracted considerable experimental and theoretical attention. Among those properties that are much studied by theoreticians are the radiative lifetimes of its excited states. Experimentally, a number of determinations of the radiative lifetimes of different excited states of helium have been made using very different experimental methods. However, in several cases these experimental determinations disagree by amounts greater than their quoted uncertainties, even when the same experimental method was used, and sometimes even with the same apparatus. Furthermore, many experimental results disagree as well with the theoretically calculated lifetimes.[1-3]

An overview of the situation can be seen by examining the cases of the 3^1S, 3^1D, and 4^1D lifetimes. The same three lifetimes were determined in the present experimental investigation. One of the least-studied states is the 3^1S state. Measurements have been performed using two methods: the delayed-coincidence method,[4-6] hereafter referred to as the DCM, and the electron-photon coincidence method,[7] hereafter referred to as the EPC method. On the other hand, the 4^1D state lifetime has been measured by six methods: the DCM,[4-6,8-15] the Hanle method,[16-18] the curve-crossing method,[19-23] the EPC,[7,24] the beam-foil method,[25] and the gas target method.[26] The measured lifetimes varied from 30 nsec (Ref. 5) to 47 nsec,[14] compared to the theoretical lifetimes of 37.8 nsec (Ref. 2) and 36.63 nsec.[8] Intermediate between these two extreme cases is the 3^1D lifetime which has been studied using the DCM,[4-6,8,10,13,14,27] the Hanle method,[1,7,18] the curve-crossing method,[19-23,28] and the EPC method.[7] The experimental lifetimes varied from 12 nsec (Refs. 22 and 24) to 22 nsec.[4] The theoretical values are 15.4 nsec (Ref. 2) and 15.6 nsec.[1]

In the present investigation the delayed coincidence method was used for remeasurements of the lifetimes of the 3^1S, 3^1D, and 4^1D states, to measure the experimentally undetermined lifetimes of the 4^1F and 5^1F states, and in the course of this work to investigate systematically many of the different factors that have contributed errors to the measured lifetimes. Some of these factors have been neglected in previously published investigations. Particular attention has been paid to the effects of incident electron-beam energy, electron-beam current, target pressure, cascades, and methods of fitting the decay curves to exponentials. In contrast with common practice,[4] where the electron-beam energy is set just above the excitation energy threshold of the state being studied, a wide range of electron-beam energies, much larger than the threshold energy, was used. It was found that cascade components can be quite small at large incident energies, and that high-beam energies can be used to advantage if the cross sections for excitation are maximum at such energies. Furthermore, in several cases cascade components could be analyzed reliably to determine the lifetime of the cascading state.

A description of the apparatus used is given in Sec. II. The experimental procedure and details of the systematics are described in Sec. III. The data processing method is described in Sec. IV. The results for the different lifetimes, a comparison with other determinations, and a critique of the different results are presented in Sec. V.

II. APPARATUS

The apparatus used to measure the lifetime of the excited states of helium consisted of a vacuum chamber and an electron gun originally described by Long *et al.*,[29] an optical system developed by Khayrallah,[30] and an electron pulsing system and photon-counting apparatus briefly discussed by Khayrallah and Smith.[31] A schematic diagram of the apparatus is shown in Fig. 1. Briefly, the experiment consisted of scattering a pulsed electron beam from a helium static gas target, and counting photons in selected atomic helium fluorescence lines as a function of time delay from the

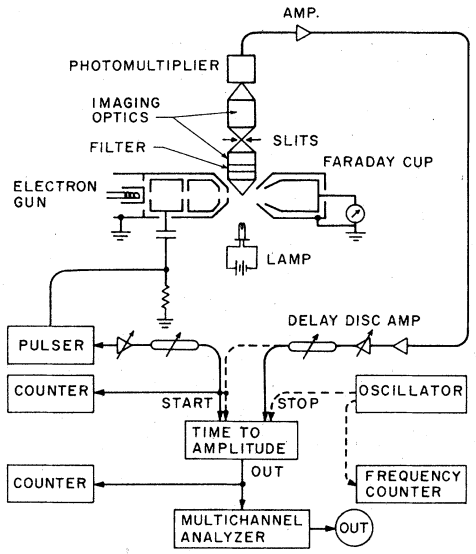

FIG. 1. Schematic diagram of the apparatus used to measure the helium lifetimes. Two sets of lines are shown connecting the different electronics boxes. The dashed lines are the modified connections used when calibrating the time response of the data acquisition system.

sharp electron-beam cutoff.

The pulsed electron beam was produced by pulse modulation of the grid of a Soa-type electron gun[32] with an indirectly heated type-A Phillips cathode. The grid was normally biased at -10 V relative to the cathode, so that the gun was cut off. A properly coupled and tailored +50-V pulse, 60 nsec long, biased the gun to generate an electron pulse approximately 60 nsec long. Part of the output of the pulser was shaped through a fast trigger discriminator, delayed through a 50-Ω delay cable, and used as a start signal for time-to-pulse height converters (TAC). Typically the electron gun was modulated at 200 kHz, with an average current of 0.21 μA, corresponding to a peak current of 13.5 μA, or approximately 5×10^6 electrons per pulse.

Radiation from the interaction region was viewed by a dry-ice-cooled RCA 31034A photomultiplier, through appropriate interference filters, and imaging optics.[30] Three interference filters were used, with peak transmissions at 667.8, 728.1, and 494.0 nm and half-band width of 10.0 nm each for the $3\,^1D$, $3\,^1S$, $4\,^1D$ radiation, respectively. These filters were three-cycle interference filters blocked to 10 μm in the infrared as well as blocked for the ultraviolet. The full width at 1% transmission was about 17.5 nm in each case. The effects of nearest lines are discussed in Sec. V below. The output pulses from the detector, ~8 nsec wide, were amplified, discriminated, and shaped by a fast trigger module, and fed to the stop input of the TAC. The output of the TAC was fed to a multichannel analyzer and its corresponding data acquisition system.

The interaction region was shielded by two layers of magnetic shielding, thus reducing the magnetic fields to less than 10 mG. The base pressure of the vacuum chamber was 8×10^{-9} Torr [$\sim1\times10^{-6}$ Pa] with titanium pumping. The pressures were measured by a nude millitorr gauge, and/or a conventional ionization gauge. The correction factor for helium sensitivity was taken to be the same for both gauges. The helium used was research grade helium with specified purity 99.9995%.

III. EXPERIMENTAL PROCEDURE

In analyzing measurements of lifetimes based on the time-delayed-observation method various sources of error must be evaluated. The main electronic errors are due to differential nonlinearity in the time scale,[4,33] calibration errors in the time scale, saturation of the counting electronics (i.e., loss of counts caused by overlapping pulses), limited definition of pulse arrival times, and channel width instability. Photomultiplier errors include variation with wavelength of the time response of the detecting photomultiplier,[34-37] effect on the pulse-height distribution of gain changes in the photomultiplier, and transit-time broadening. Other experimental errors are due to cascading, stray electromagnetic fields, resonant radiation trapping, space-charge effects, collisional deexcitation, and excited atom drift in and out of the field of view of the detector. Finally, errors due to the method of extraction of the decay constants from the data are present, and they should not be treated lightly. This section describes the efforts made to correct, avoid, measure, or estimate these errors.

A. Electronics

In order to calibrate the time scale, one must measure absolutely the elapsed time at each channel, as well as the individual channel width Δt_i for the discriminator, time-amplitude converter, plus multichannel analyzer combination. The method used was a modification of that described by Baker *et al.*[38] and by Lawrence.[33] This method not only allows an absolute measurement of the time scale, but it also allows the measurement of the differential nonlinearities among the channel widths. For this measurement, the start and stop signals to the TAC were modified as indicated in Fig. 1, and the electron-gun heater was disconnected so that no electron current flowed into the interaction region. An incandescent lamp was

placed in front of the photomultiplier and its intensity was adjusted by varying its direct current to give a few tens of kilohertz random count rate. The stop pulses are uniformly spaced with a period T, as measured by a stabilized frequency meter, so that the random start pulses form random time intervals distributed uniformly between zero and T. Hence the number of the true stop pulses n_i in channel i is proportional to the width of the channel Δt_i. In particular $\Delta t_i = n_i T/N$, where N is the total number of stop pulses counted by a 100-MHz scaler. In this method the time period T is also calibrated on the time scale of the instrument, since no count should occur after the channel corresponding to time T.

In the present investigation the TAC was disabled for 10 μsec after every coincidence between its start and stop pulses. Thus N is a true measure of the stop pulses. In general it was found that the number of true coincidences to the number of input start pulses was unity to better than 0.01%. The counting in this system was arranged so that n_i were accumulated to about 9×10^4 counts, thus giving 0.3% rms random error per channel. The maximum differential nonlinearity was found near the beginning and the end of the range, and usually amounted to less than 4%. This is larger than the manufacturer quoted value of 2% for the TAC and is due to the nonlinearity in the multichannel-analyzer conversion. During the present experiment the range was confined to the region where the differential nonlinearities were less than 2%.

Two checks were made on the determinations of Δt_i. First, Δt_i was determined as a function of both T and the random arrival rate. It was found that Δt_i did not vary by more than 0.5% for T^{-1} varied to greater than 10 MHz and random pulse rate up to 100 kHz. A second check was to measure the integral linearity of the system through the determination of the absolute value of time difference between different channels. A very stable frequency-adjustable oscillator was fed to both discriminators just ahead of the inputs of the TAC, but with a small arbitrary delay of 1 nsec in the start channel. For an input frequency corresponding to period T_i, the counts will be accumulated in a channel i. The time difference t_{ij} between channels i and j is $t_{ij} = |T_i - T_j|$, where T_i and T_j are the periods necessary to count in channels i and j, respectively. Using Δt for channel width, one can write

$$t_{ij} = \sum_{l=i+1}^{j-1} \Delta t_l + \tfrac{1}{2}(\Delta t_i + \Delta t_j) . \qquad (1)$$

It was found that both methods agree to within $\pm 1\%$ and that the maximum integral nonlinearity was less than 0.1%. Thus the time scale was calibrated absolutely to an accuracy of better than 0.5%.

B. Detector

Timing errors and uncertainties introduced by the detector can be classified under three sources: (a) transit-time variation, (b) variation with cathode area, and (c) wavelength variation of the detector-transit-time response. For the present photomultiplier (RCA 31034A) the single-photoelectron transit-time spread given at the half-amplitude points of the anode output pulse was measured to be 7 nsec, while the pulse rise time was measured to be 2.5 nsec. Both measurements were made when the full cathode was illuminated and represent the worst case conditions for timing.[39] A more severe timing problem was due to the variation of the pulse-height amplitude, and hence the timing of the trigger pulse of the discriminators. However, a very high electronic gain (of approximately 1000) was used such that when the discriminator level was varied, no effect larger than a 1% variation on the short lifetimes was seen. This corresponds to 300-psec walk, no larger than a constant fraction timing discriminator should give. The walk effect is due to an inherent dependence of the photomultiplier time response (both rise time and spread) on the anode current.[39]

Timing error due to the variation of the response time with wavelength has been observed by many.[34-37] The main errors were found when measuring short lifetimes (< 10 nsec) and corresponded to less than one-half a nanosecond variation in those lifetimes.[34] No effort was made in the present investigation to study this effect.

C. Geometric loss

Another detection error arises from the failure to detect long-lived excited atoms that diffuse out of the field of view of the detector. In the present case the exciting electron beam had a 1-mm full width at half-maximum (FWHM) while the detection optics had a variable field of view extendable up to 1 cm. If one uses a simple model for diffusion[30] where all the helium atoms move at an angle ψ relative to the optics axis with a velocity v, then the fraction of the atoms not seen by the detector $L(\sigma)$ is given by

$$L(\sigma) = (\sigma/w) e^{-(\Delta/\sigma)} \sinh(w/\sigma) , \qquad (2)$$

where $\sigma = vT \sin\psi$, T is the lifetime of the state, Δ is the field of view, and w is the full width of the electron beam. For a helium atom with a thermal velocity of 1.5×10^3 m sec^{-1}, a 2-mm field of view, and a 1-mm electron-beam FWHM, the worst

loss is less than 1% for an atom with a lifetime of 100 nsec, moving at angle of 90° with respect to the optics axis. Of course not all of the atoms diffuse out of the viewing volume at an angle of 90°, and an average over ϕ should be made

$$\langle L(\sigma)\rangle = \frac{\int_0^{\pi/2} L(\psi)d\psi}{\int_0^{\pi/2} d\psi} = \frac{vT}{w\pi}\frac{\Gamma(\frac{1}{2})}{\sqrt{\pi}}\left[\int_\beta^\infty \int_\beta^\infty K_0(\beta)\,d\beta - \int_\mu^\infty \int_\mu^\infty K_0(\mu)\,d\mu\right], \tag{3}$$

$$\mu = (\Delta - w)/vT, \tag{4}$$

$$\beta = (\Delta + w)/vT, \tag{5}$$

where K_0 is the modified Bessel function of order zero, and the integral can be done numerically. For the same parameters used above the loss becomes 0.1%. However, we should also consider that a helium atom recoils when it is excited by an electron of energy E. The recoil velocity is given by

$$v = \frac{m}{M+m}\left[\cos\theta \pm \left(\cos^2\theta - \frac{m+M}{M}\frac{\Delta E}{E}\right)^{1/2}\right]v_e, \tag{6}$$

where m and M are the electron and helium masses, respectively, v_e and v are the electron and helium velocities, respectively, θ is the recoil angle, and ΔE is the excitation energy. For 500-eV electrons the maximum recoil velocity, 3.58×10^3 m sec^{-1}, is in the forward direction. The corresponding loss amounts to ~0.3%. Since all the measured lifetimes were shorter than 100 nsec, the geometric detection loss is negligible as a source of error in the present experiment.

D. Perturbing effects

Included in this category are resonant radiation trapping, space-charge effects, collisional deexcitation, and effects of stray electromagnetic fields. In order to reduce the effect of resonant radiation trapping, emission from the excited states was observed only for transitions to the short lifetime $2\,^1P$ states. In addition the pressure of the helium target was kept below ~10^{-5} Torr (~10^{-3} Pa), where the effects of collisional deexcitation and excitation transfer can be neglected. For pressures below 10^{-5} Torr it was found that the measured lifetimes did not depend on the pressure.

External electromagnetic fields were also minimized in the collision region by the use of magnetic shielding and coating of the collision region with Aquadag. Magnetic fields were measured, using a Hall probe, to be less than 10 mG (10^{-6} T). No method as yet exists to measure the actual electric field directly, but a previous indirect measurement using the effect of electric fields on the measured lifetime of the $3s$ state of atomic hydrogen established a limit of less than 2 V m^{-1}.[30,31]

The influence of the space charge of the electron-beam current was also studied by varying the peak electron-beam current and examining the measured lifetimes. No effect was observed for electron-beam peak currents less than 14 μA. At the electron-beam current and helium pressure used, and for the case of high-energy electron impact, it is also expected that the positive-ion density was too small to have had an effect.

E. Cascades

It is inevitable that cascades should influence the measured lifetimes and contribute to the measured intensity, except for those methods based on detection of a coincidence between an exciting scattered electron and the delayed photon[40] or on detection of an exciting photon and the delayed photon in cascade.[41] Bennett *et al.*[4] suggested that in order to eliminate cascades the exciting electron beam be operated just above the threshold for excitation of the observed state. Bennett's suggestion works for low-lying states that are separated by an energy less than the spread in the electron-beam energy. However, by operating at threshold where excitation cross sections usually are small one may face severe signal-to-noise problems, especially when operating at very low target pressures and electron-beam currents.

In the present study another approach was followed. The lifetimes of the states were also measured as a function of incident electron-beam energy from threshold to 500 eV. The decay rates of cascades could be separately identified and measured. The size of cascade components could be estimated. Furthermore, an enhancement in the signal-to-noise ratio, as well as an increase in the signal rate was obtained at higher energies. In the present experiment most of the cascades originated from the $n\,^1P$ states, and from the $n\,^1F$ states. The $n\,^1P$ states, including the effects of imprisonment, have very short lifetimes relative to the presently measured lifetimes and they also have a small branching ratio for radiating to states other than the $1\,^1S$ state. Thus, with care, one can safely neglect the effect of the $n\,^1P$ states. The $n\,^1F$ states, however, are longer lived than the $n\,^1D$ states, and although their excitation probability is small, one should include their effect in the $n\,^1D$ state analysis since they can decay only through the $n\,^1D$ states. An estimate of the branching ratios and the fractional contributions due to cascade are presented in Table I for the

TABLE I. Fractional contributions from cascades to the measured $3\,^1S$, $3\,^1D$, and $4\,^1D$ decay at 100 eV and at zero time after the excitation. Calculated from Eq. (9).

Final state n	Cascading state J	Branching ratio ×100 (Ref. 1)	σ_J/σ_n (Ref. 41)	Contribution ×100
$3\,^1S$	$4\,^1P$	0.498	4.00	−2.145
	$5\,^1P$	0.956	2.03	−2.25
	$6\,^1P$	0.749	···	···
$3\,^1D$	$4\,^1P$	0.181	6.28	−1.51
	$5\,^1P$	0.055	3.18	−5.7
	$4\,^1F$	100	0.05	+1.15
	$5\,^1F$	64.3	···	···
$4\,^1D$	$5\,^1P$	0.166	6.69	−1.40
	$6\,^1P$	0.122	···	···
	$5\,^1F$	36.0	···	···

$3\,^1S$, $3\,^1D$, and $4\,^1D$ states. The fraction is given by

$$f=(\sigma_j/\sigma_n)[A_{jn}/(A_n-A_j)], \tag{7}$$

where σ_i is the cross section for exciting state i, A_{jn} is the transition probability from state j to state n, while A_n is the total decay rate of state n. (See Sec. IV A for details.)

F. Electron pulse shape

An important contribution to systematic errors is the decay tail of the exciting electron pulse. A common error is the assumption that the electron current pulse is proportional to the modulating voltage pulse applied to the electron gun. In the present study a direct measure of the shape of the electron pulse was made using two separate methods. In the first method, the photomultiplier looked at the 501.6-nm emission from the $3\,^1P$ state of helium through a narrow-band interference filter with peak transmission at 504.7 nm and FWHM of 10.0 nm. The $3\,^1P$ state has a 1.726-nsec lifetime.[1] Although some cascade contributes to the signal, especially from the $4\,^1S$ and $4\,^1D$ states with lifetimes of 89 and 36 nsec, respectively, this contribution to the signal is very small, since the cross sections for excitation of the $4\,^1S$, $4\,^1D$, and $3\,^1P$ states were measured to be 7.7, 6.75, and 260×10^{-20} cm^2, respectively,[42] at 100-eV incident-electron energy. Thus one can deconvolute the data using program FIT (to be described in Sec. IV) to get an estimate of the electron pulse shape in the interaction region. The second method relied on measuring the Bremsstrahlung radiation[31,43] resulting from the electron-beam impact on a silver target positioned in the interaction region and inclined at 45° to both the electron-beam axis and the optics axis. It is expected that this Bremsstrahlung radiation, also called transition radiation in Ref. 43, is instantaneous. Due to the spread in velocities of the incident electron beam and the consequent variation in transit time through the surface, a smearing in the time sampling of this instantaneous radiation occurs. For the measured beam energy spread of $\Delta E=0.35$ eV at a beam energy $E=100$ eV and corresponding smearing time ΔT is

$$\frac{\Delta T}{T}=\frac{\Delta V}{V}=\frac{1}{2}\frac{\Delta E}{E}=\frac{1}{600}, \tag{8}$$

where T is the pulse width. For $T=60$ nsec the smearing corresponds to 0.1 nsec.

The decay time of the electron pulse was measured. It took 15 nsec for the electron-beam amplitude to fall to a level of 0.1% of its full amplitude. The accuracy in time for the determination of the position of this 0.1% level was less than 1 nsec.

All fits were based solely on data taken after the electron pulse had decayed to less than 0.1% of its full amplitude. Additional excited-state population contributed by the tail of the electron pulse was negligible. Thus the lifetime measurements were properly based on pure radiative decay of a well-determined initial excited-state population, according to Eq. (9) below.

IV. DATA PROCESSING

This section describes the methods used in extracting meaningful lifetimes from the data, and the precautions taken. First, the functional form of the decay is discussed, and then the fitting procedure is described.

A. Functional form of the measured decay

A state n with lifetime τ_n decays exponentially in time such that the instantaneous population (and hence emitted intensity) is given by

$$N_n(t)=N_n(0)e^{-\alpha_n t}+\sum_{j\to n}N_j(0)A_{jn}\left(\frac{e^{-\alpha_n t}}{(\alpha_j-\alpha_n)}+\frac{e^{-\alpha_j t}}{(\alpha_n-\alpha_j)}\right), \tag{9}$$

where the only cascades included are directly from states j to state n. A_{jn} is the transition probability for cascade from $j\to n$, α_n is the inverse mean life of level n, and where $N_i(0)$ is the initial population of the state i. However, since the experiment counts the decay in a unit time ΔT_i in channel i, the measured decay count in channel i is given by

$$C_n(i)=\int_{t_i-(1/2\Delta T_i)}^{t_i+(1/2\Delta T_i)}N_n(t)\,dt, \tag{10}$$

so that every exponential factor is replaced by

$$e^{-\alpha_n t_i}\to\Delta T_i\frac{\sinh\frac{1}{2}\alpha_n\Delta T_i}{\frac{1}{2}\alpha_n\Delta T_i}e^{-\alpha_n t_i}. \tag{11}$$

For very small channel width ΔT_i

$$e^{-\alpha_n t_i} \to \Delta T_i e^{-\alpha_n t_i}. \tag{12}$$

In general one can replace t_i by $t_i = ik$, where k is the average time per channel. Thus the final form of the observed decay is given by

$$I_n[i] = a_{ni} e^{-\beta_n i} + \sum_{j \neq n} a_{ji} e^{-\beta_j i} + a_0, \tag{13}$$

where

$$a_{ji} = \frac{N_j(0) a_{jn}}{\alpha_n - \alpha_j} \frac{\sinh \frac{1}{2}\alpha_j \Delta T_i}{\frac{1}{2}\alpha_j \Delta T_i} \Delta T_i, \tag{14}$$

$$a_{ni} = \left(N_n(0) + \sum_{j \neq n \neq 0} \frac{N_j(0) A_{jn}}{(\alpha_j - \alpha_n)} \right) \frac{\sinh \frac{1}{2}\alpha_j \Delta T_i}{\frac{1}{2}\alpha_j \Delta T_i} \Delta T_i, \tag{15}$$

$$a_0 = (\text{constant background}), \tag{16}$$

and

$$\beta_j = k/\tau_j = \alpha_j k. \tag{17}$$

Usually a fit is made for all a's and β's. Then using the value of k and its variance σ_k (one standard-deviation error) we see that each lifetime is given by

$$\tau = k/\beta, \tag{18}$$

and its relative variance by

$$\frac{\sigma_\tau}{\tau} = \frac{1}{\tau}\frac{\partial T}{\partial k} + \frac{1}{\tau}\frac{\partial T}{\partial \beta} = \frac{\sigma_k}{k} + \frac{\sigma_\beta}{\beta}. \tag{19}$$

Finally, the lifetime and its confidence interval are given by

$$\tau \pm \sigma_\tau t_{(\beta/2,\nu)}. \tag{20}$$

Here the $t_{(\beta/2,\nu)}$ corrects for the finite number of degrees using a Student's t distribution with ν degrees of freedom and $100(1-\beta)\%$ confidence level. For most of the present results $t_{(\beta/2,\nu)} = 2.25$ for 95% confidence level.[44]

One notes that an effect of jitter in the timing translates into a random smoothing of the data again with a weight ΔT_i. Thus inclusion of the effect of the channel width is of the utmost importance in getting a reliable estimate of the lifetime.

B. Fitting errors

To calculate the observed decay rates (and hence lifetimes) from the measured data, three different calculation methods were used with variable success. The first, and the simplest, was a combination of a graphical and computer technique called **FIT**. The longest lifetime was determined first, then its contribution to the decay was subtracted. The cycle was repeated, until one finally found the instrumental response of the system. It was found that this technique suffered from a lack of an estimate of the uncertainties. Hence the technique was used to establish close guesses. The second technique was to use a least-squares fit to a nonlinear function of the lifetimes with a linearization of the fitting function using Marquard's algorithm.[45] The computer program was the **CURFIT** routine given by Bevington.[46] One of the advantages of this technique is its speed and ability to converge in few iterations to one unique result with an error estimate. However, it quite often gave accurate lifetimes whose standard deviations were too small, smaller than the expected difference between the test values and the fitted values. The third procedure used least-squares nonlinear fitting routines **DSPAK** implementing Gauss' iterative method.[47] **DSPAK** tended to be very sensitive to the original guesses and took many steps to converge. However, **DSPAK** tended to give quite accurate estimates of the uncertainties in the fit, as well as an estimate of the standard deviation of the predicted mean. The final procedure for fitting was to use **FIT** to generate a guess. Then **CURFIT** was used to generate a good estimate from different guesses. Finally with **DSPAK** we obtained a final estimate of the lifetimes, contributions, and their absolute uncertainties.

The procedure was studied exhaustively by generating a wide range of test cases with variable random uncertainties. It was found that the present procedure can untangle three exponentials correctly, provided the random noise was less than 5.0% of the input data. This forced counting a minimum of 2000 counts per channel. Typically the peak count was above 10 000 counts. The minimum count was limited by the decay time. Generally, 25–100 channels were used in the fit, corresponding to a period at least as great as three mean lifetimes of the state. The fit was usually made for an increasing number of exponentials until a minimum in the normalized residuals was found. That fit was assumed to give an unbiased estimate. An attempt was made to introduce logarithmic smoothing into the procedure. Logarithmic smoothing tended to reduce the uncertainties and the residuals. However, it did not change the lifetimes. The logarithmic smoothing procedure consisted of replacing $C(i)$ by $\bar{C}(i)$

$$\bar{C}(i) = \left[\prod_{J=i-(N/2)}^{J=i+(N/2)} C(J) \right]^{1/(1+N)}, \tag{21}$$

where $C(i)$ is counts in channel i, i is the channel number, N is the order of smoothing, and $\bar{C}$ is

the new smoothed result. A rigorous treatment of this procedure showed that the new set of smoothed data contained the same lifetimes, but with different contributions. Logarithmic smoothing helped establish a confidence in the fit, but was not used in obtaining the final results.

Usually, the number of fitted points, the initial channel number, as well as the number of exponentials were varied in order to understand the behavior of the data. Typically, the value of the estimated lifetimes given by DSPAK and CURFIT agreed to at least three decimals.

C. Example

In this section we examine one set of data (for $3\,^1S$ decay at 728.1 nm) and show some of the results of the analysis. In Table II one can see the effects of varying the number of points (or region of fit), as well as the effect of varying the number of exponentials. As the region of the fit was expanded, a worsening of the results of the single exponentials was evident. As the number of exponentials was increased, χ^2 (the normalized sum of residuals) decreased, the absolute error estimates were increased, and the magnitude of β_1 (the largest component) settled to within 1%. By looking at the total fit, however, one cannot easily distinguish between the last four fits. Figure 2 displays the fit, and Fig. 3 displays the residuals as well as the predicted deviation from the mean for one exponential fit. In Fig. 3, one notes the lack of a fast component ($\beta=2$) in the fit as evidenced by the large residuals at small times. It should be made clear that the residuals plotted are absolute differences, not weighted, and that the residuals are smaller than the variance of the input data at small times.

V. MEASURED DATA AND DISCUSSION

The results of the present measurements of the radiative mean lifetimes of the $3\,^1S$, $3\,^1D$, and $4\,^1D$ states of helium are shown in Figs. 3, 4, and 5, respectively. The error bars shown for the present measurement are at the 95% confidence level and include errors due to fitting, counting uncertainties, differential nonlinearities, and timing calibration. The figures also show the lifetime measurements of other investigators. What follows in this section are discussions of each lifetime determination.

A. $3\,^1S$ state

The only single-photon decay-channel available for the $3\,^1S$ state of helium is an electric dipole transition to the $2\,^1P$ state of helium with a wavelength of 728.1 nm. Within the 10.0-nm band pass of the interference filter used in the present study, no other helium lines were transmitted by the interference filter. The nearest lines were the $3\,^1D \rightarrow 2\,^1P$ (667.8 nm) and $3\,^3S \rightarrow 2\,^3P$ (706.5 nm) lines. Single-stage cascades to this level could occur from the $4\,^1P$, $5\,^1P$, and $6\,^1P$ states with approximate lifetimes of 4, 7.5, and 13 nsec, respectively.[1] Less than 2% of the decay at short times for electron energies of 100 eV should be caused by cascade from each $n\,^1P$ state (see Table I, for example). Multiple-stage cascade contributions would be much less than 2% due to their unfavorable excitation cross sections and their small branching ratios (most would go to the $2\,^1P$ state). In the actual fits the contribution of the $4\,^1P$ state was found to be $4 \pm 1\%$ at 500 eV. A very long lifetime with very small amplitude contribution was also found but could not be identified with any known state. As can be noticed from Table II the

TABLE II. Variation of the fitted parameters as a function of number of points in the fit and the number of fitted parameters. Data for $3S$ decay. Average time per channel 6.6448 ± 0.0366 nsec. The numbers between brackets are the estimated variances of each estimate of the mean value of the parameter.

No. of points	a_1	β_1	a_2	β_2	a_3	β_3	a_0	χ^2_2
25	76 700(74)	0.118 89(11)	•••	•••	•••	•••	−97(18)	13.5
40	76 701(140)	0.120 74(26)	•••	•••	•••	•••	209(17)	9.1
55	76 710(136)	0.120 79(20)	•••	•••	•••	•••	215(6)	7.6
70	76 689(133)	0.120 70(18)	•••	•••	•••	•••	209(3.5)	8.34
85	76 544(116)	0.120 24(15)	•••	•••	•••	•••	187(2.3)	11.38
100	76 463(131)	0.119 89(17)	•••	•••	•••	•••	177(2)	12.23
100	77 001(184)	0.120 50(2)	−3338(327)	2.21(0.83)	•••	•••	183(2)	4.13
100	76 298(132)	0.120 73(20)	•••	•••	206(20)	0.0107(0.0197)	90(15)	4.7
100	77 404(191)	0.122 2(3)	−3949(343)	2.17(0.93)	292(61.8)	0.0189(0.0118)	117(27)	0.5

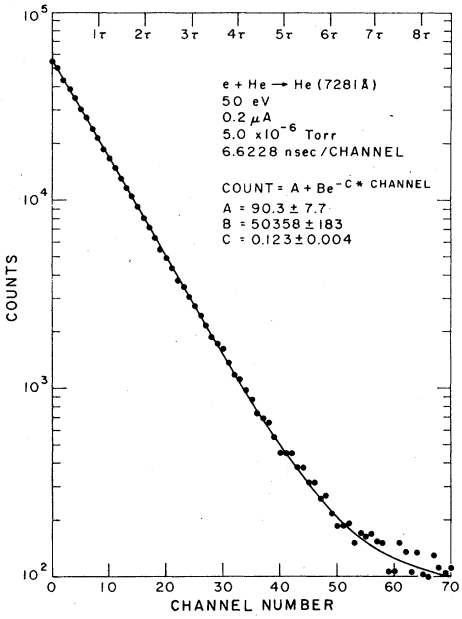

FIG. 2. Plot of the decay of the 728.1-nm radiation following a 60-$n$sec long, 50-eV electron pulse. The solid dots represent the observed counts and the solid line a single exponential fit to the data. The top axis represents time in units of measured lifetime τ of the $3\,^1S$ state of helium.

sign of the $4\,^1P$ contribution is negative. This is in accordance with the physical picture for the direct cascade contribution from a level with shorter lifetime than the fed level (Table I). The $4\,^1P$ lifetime was determined from our fit to be 3.02 ± 1.5 nsec in agreement with the much more precise measurements[18] and the theoretical value

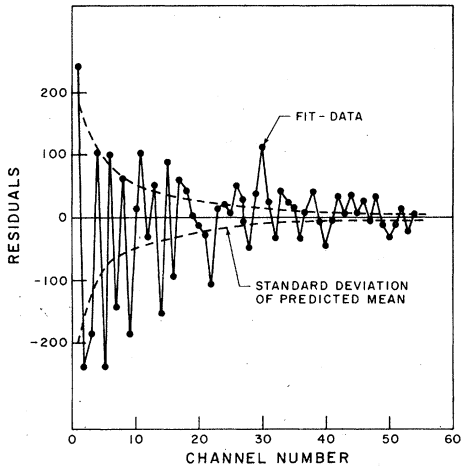

FIG. 3. Plot of the residuals of the fit in Fig. 2. The solid dots are the absolute unweighted residuals; the dashed line is the calculated estimate of the standard deviation of the predicted mean.

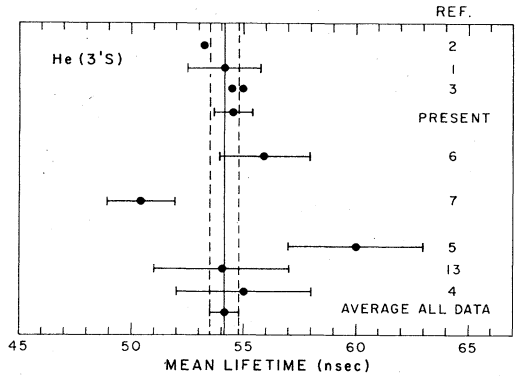

FIG. 4. Scatter plot of the different determination of the He($3\,^1S$) mean lifetime. The error bar on the present data represents the 95% confidence level. The dashed line represents the 95% confidence interval for the average of all experimental results.

of 3.93 nsec.[1-3] The $3\,^1S$ lifetime was measured at 50 and 500 eV. Table III lists the determinations at 500 eV for different values of current and pressure and is indicative of the spread within the data. The average value of $3\,^1S$ lifetimes was found to be 54.9 ± 0.9 nsec at 500 eV and 53.9 ± 0.9 nsec at 50 eV. The weighted average value of the two was 54.5 ± 0.8 nsec.

As can be seen from Fig. 4, there have been very few lifetime measurements on the $3\,^1S$ state. Before the present measurement, three measurements[4,5,13] using the present technique were made. Results of Ref. 5 were larger than the others. An electron-photon coincidence measurement[7] was in poor agreement with those three results. Since then, the method of Holzberein[11] was used,[6] with the results favoring Bennett *et al.*'s results. The present result also agrees with Bennett *et al.*[4,13]

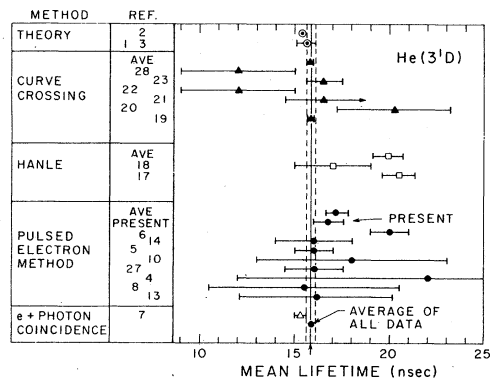

FIG. 5. Scatter plot of the different determinations of the He($3\,^1D$) mean lifetime. The error bar on the present measurement represents the 95% confidence interval. The weighted average of each method is shown within each group of measurements. The vertical dashed lines enclose the 95% confidence interval for the weighted average of all experimental results.

TABLE III. Measured decay constant for the $3\,^1S$ state at 100 eV. The average time per channel is 6.6448 ± 0.0366 nsec.

Run no.	Decay constant (channels^{-1})	σ (channels^{-1})
77	0.123 81	8.45×10^{-4}
78	0.120 85	3.39×6^{-4}
79	0.122 31	7.09×0^{-4}
80	0.120 74	2.68×0^{-4}
Average	0.121 06	1.96×10^{-4}

The theoretical results are shown as well in Fig. 5. The estimated uncertainty in the Wiese *et al.* result is 3%.[1] No comparable uncertainty exists for Gabriel and Heddle's value[2] or for the results of Green *et al.*[3] The weighted average of all the experimental results (the weight used was $1/\sigma^2$, σ being the quoted error) is 54.2 ± 0.6 nsec in agreement with the theoretical results. Two experiments[5,7] are far from the weighted average. Neglecting those two experiments does not change the weighted average considerably. The present result agrees very well with the weighted average as well as with the theoretical results.

B. $3\,^1D$ state

The $3\,^1D$ state of helium decays either to the $3\,^1P$ or the $2\,^1P$ state with the emission of a single photon at 95760.0 or 667.8 nm, respectively. In the present experiment the visible photon at 667.8 nm was detected. Within the band pass of the interference filter used, no other helium line is observed by the detection system. Single-stage cascades to the $3\,^1D$ state could occur from the $4\,^1P$, $5\,^1P$, $n\,^1P$, $4\,^1F$, $5\,^1F$, and $n\,^1F$ states. Using the measured cross sections for excitation of the $4\,^1P$, $5\,^1P$ states,[42] and the $4\,^1F$ state[48,49] at 100 eV, one finds from Table I that less than 1.5% of the $3\,^1D$ state emission at short times ($\leq$2 nsec) comes from the $4\,^1P$ state, and that the $4\,^1F$ state contributes appreciably for very large times after the excitation.

In the experiment it was found that for all energies the amount of cascade was small, especially beyond the time for which the statistical fluctuations became significant. The present data could not resolve the very short-lived $n\,^1P$ contributions. Generally two cascades with lifetimes of 67 ± 10 nsec and 142 ± 20 nsec were present in the measured decay curves. The 67-nsec contribution could be identified with the cascade from the $4\,^1F$ state. No previous measurement of $4\,^1F$ state has been reported; however, theoretical calculations give 72.36 nsec[1,2] to an accuracy of ±10%.[1] The 142-nsec component could be identified as originating from the cascade from the $5\,^1F$ state whose theoretical lifetime was calculated to be 139 nsec ±10%[1] and 143 nsec.[2] Again no comparable measurement exists. It is interesting to compare the measured helium F-state lifetimes with the atomic hydrogen F-state lifetimes. For large angular momenta one could expect similar values, and indeed the hydrogenic $4F$ and $5F$ lifetimes are 73 and 140 nsec, respectively.

TABLE IV. Lifetime of the $3\,^1D$ state of helium for different energies. σ is one standard deviation error.

Energy (eV)	T (nsec)	σ_T (nsec)
30	17.17	0.17
40	16.66	0.125
50	16.44	0.151
82	16.61	0.166
122	16.48	0.168
200	16.47	0.205
300	16.90	0.170
500	17.06	0.160
Average	16.71	0.72

The results of the present lifetime determination of the $3\,^1D$ state as a function of energy are listed in Table IV. It is evident that no systematic trends exist in the data. The weighted value of fitted lifetime was 16.7 nsec. One standard deviation is ±0.1 nsec. However, for 95% confidence the error in the fit was 2.25 σ = 0.3 nsec. Since the error in the calibration of the time was very large for these very short lifetimes, one should add linearly the absolute error in the local integral nonlinearity and differential nonlinearity ($\simeq$0.5 nsec) to get a final estimate $\tau_{3\,^1D} = 16.7 \pm 0.8$ nsec.

A comparison of the present result with the different experimental and theoretical results is shown in Fig. 5, where results from each method are grouped together. The weighted average of the pulsed electron technique (not including the present measurement) is 17.2 ± 0.6 nsec. The present measurement agrees with this average. Only one measurement using this technique disagrees with this average[6] as well as with the present measurement. However, note that most of these measurements, with the exception of the present measurement, have used relatively high pressures ($>5\times10^{-3}$ Torr).

The electron-photon coincidence technique[7] was also used to measure the $3\,^1D$ lifetime. However, that measurement disagreed with the pulsed-electron-beam method.

Other techniques not involving direct measurement of time include the Hanle effect[17,18] as well

as the curve-crossing techniques.[19-23,28] The weighted average of the Hanle effect is quite far from the mean of the data and the theory. However, it is interesting to note the large scatter in the curve-crossing results, as well as the nonagreement within their estimated uncertainties, even when the lifetimes were measured by the same author. The average of the curve-crossing technique, as well as for all the experimental data, is weighted very heavily by the small uncertainty in Buchaupt's[19] determination.

The theoretical results, 15.7 ± 0.5,[1] 15.4,[2] 15.68 nsec,[3] in the length approximation and 15.71[3] in the velocity approximation, are in agreement with the total weighted average of all the experimental results (15.8 ± 0.2 nsec) as well as with the present results.

C. $4\,^1D$ state

The $4\,^1D$ state can decay to either the $3\,^1P$ or $2\,^1P$ state with the emission of a single photon at 1908.9 or 492.2 nm, respectively. In the present experiment the visible photon at 492.2 nm was detected. The interference filter, however, has a transmittance of $< 3\%$ at the $3\,^1P - 2\,^1S$ (501.5 nm) radiation. The mean lifetime of the $3\,^1P$ decay is 1.7 nsec. Furthermore, although the cross section for the excitation of the $3\,^1P$ state is about 50 times larger than the cross section for the $4\,^1D$ state,[42] the product of the cross section, branching ratio, and transmission of the interference filter is in the ratio of 0.075:1 for $3\,^1P$:$4\,^1D$ contribution at the end of the electron pulse or at the beginning of the decay region. After only one channel ($\simeq 5$ nsec) the $3\,^1P$:$4\,^1D$ contribution becomes 0.006:1 and the 501.6-nm line does not interfere with the present measurement.

Cascades, on the other hand, occur from the $n\,^1F$ and $n\,^1P$ states. However, due to their small branching ratios, only the $5\,^1F$, $5\,^1P$, and $6\,^1P$ states contribute with lifetimes of approximately 140, 7.5, and 13.2 nsec, respectively. From Table I it is expected that only the $5\,^1F$ would contribute significantly.

The data were taken at 50 and 500 eV, with measured lifetimes of 37.5 ± 0.6 and 35.3 ± 0.7, respectively. The weighted average of the two is 36.4 ± 1.2, where the uncertainty is at the 95% probability level. It was found that very little cascade exists at 50 eV, but that at 500 eV a component with lifetime of 138 ± 20 nsec was present. This cascade could be identified with the $5\,^1F$ state. The present result for the $4\,^1D$ lifetime agrees quite well with the theoretical result 36.6 ± 1.8 nsec.[1] The uncertainty in the theoretical calculation was due in part to an uncertainty of 10% in the $4\,^1D$-$3\,^1P$ transition probability, and an uncertainty of 3% in the $4\,^1D$-$2\,^1P$ transition probability. The present result agrees with the theoretical results of Gabriel and Heddle,[2] 37.8 nsec, only if the present uncertainty is stretched to the 99% confidence limit. On the other hand, the present measurement agrees very well with the more recently calculated values of Green *et al.*[3] Their values were 37.04 nsec using the length calculation and 37.07 nsec using the velocity approximation for the dipole moments.

A comparison between the present and the different determinations of the $4\,^1D$ lifetime is shown in Fig. 6. The different methods are grouped together. The weighted average (not including the present result) of the pulsed electron method is 36.4 ± 1.2 nsec.[4-6,8,9,11,12,14,15] This is in agreement with the present result. However, it is evident that many of the determinations are quite far off.[5,6,12,14,15] Three determinations also exist with the Hanle method[16-18] and it is interesting that the most recent[18] disagrees with the other results and has the largest error bars. A similar behavior also exists in the curve-crossing method for the determination of the $4\,^1D$ lifetime; the most recent value[20] disagrees with the other values although it agrees with the result obtained by the same investigators[26] using a fast He^+ excitation technique. The only beam-foil measurement,[25] and the only delayed photon-electron coincidence result[7] agree quite well with the other measurements. The weighted average of the total experimental results was 37.65 ± 0.04 nsec at the

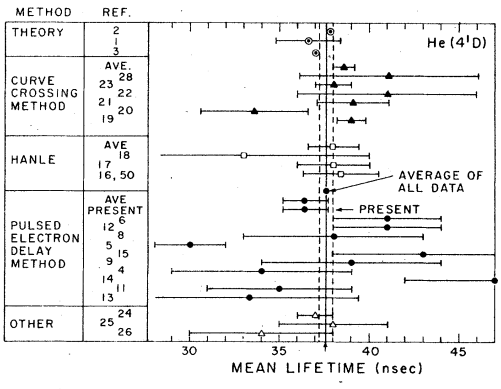

FIG. 6. Scatter plot of the different determinations of the He($4\,^1D$) mean lifetime. The error bar on the present measurement represents the 95% confidence interval. The weighted average of each method is shown within each group of measurements. The vertical dashed lines enclose the 95% confidence interval for the weighted average of all experimental results.

65% confidence level (assuming each author's uncertainties were one standard deviation).

VI. CONCLUSION

The present paper presents the results of the measurement of the $3\,^1S$, $3\,^1D$, and $4\,^1D$ lifetimes, as well as first measurements of the $4\,^1F$ and $5\,^1F$ lifetimes in helium atoms using the delayed-coincidence pulsed-electron-beam method. Particular attention has been given to estimating and discussing the different error contributions to the result. The measurement of each lifetime was discussed separately and a comparison was made with the results available in the literature.

It was found that the $3\,^1S$, $3\,^1D$, $4\,^1D$, $4\,^1F$, and $5\,^1F$ lifetimes are 54.5 ± 0.8, 16.7 ± 0.8, 36.4 ± 1.2, 67 ± 10, and 142 ± 20 nsec, respectively. These values have uncertainties smaller than those of most previous determinations. They agree with the theoretical results, as well as with the weighted average of all previous experimental results.

ACKNOWLEDGMENT

This work was supported in part by NSF grant MPS72-05169 through the University of Colorado.

---

*Present address: Dept. of Physics, Univ. of Arizona, Tucson, Ariz. 85721.

†Staff member, Quantum Physics Division, National Bureau of Standards.

[1]W. L. Wiese, M. W. Smith, and B. M. Glennon, *Atomic Transition Probabilities*, NSRDS-NBS 4 (U.S. GPO, Washington, D.C., 1966), Vol. I.

[2]A. H. Gabriel and D. W. O. Heddle, Proc. R. Soc. Lond. A 258, 124 (1960).

[3]L. C. Green, N. C. Johnson, and E. K. Kolchin, Astrophys. J. 144, 369 (1966).

[4]W. R. Bennett, Jr., P. J. Kindleman, and G. N. Mercer, Appl. Opt. Suppl. 1, 34 (1965).

[5]A. L. Osherovich and Ya. F. Verolainen, Opt. Spektrosk. 24, 162 (1968) [Opt. Spectrosc. (USSR) 24, 81 (1968)].

[6]R. T. Thompson and R. G. Fowler, J. Quant. Spectrosc. Radiat. Transfer 15, 1017 (1975).

[7]A. Pochat, M. Doritch, and J. Peresse, J. Chem. Phys. 70, 936 (1973).

[8]L. Allen, D. G. C. Jones, and D. G. Schofield, J. Opt. Soc. Am. 59, 842 (1969).

[9]K. A. Bridgett and T. A. King, Proc. Phys. Soc. Lond. 92, 75 (1967).

[10]R. G. Fowler, T. M. Holzberlein, C. H. Jacobson, and S. J. B. Corrigan, Proc. Phys. Soc. Lond. 84, 539 (1964).

[11]T. M. Holzberein, Rev. Sci. Instrum. 35, 1041 (1964).

[12]A. W. Johnson and R. G. Fowler, J. Chem. Phys. 53, 65 (1970).

[13]P. J. Kindleman and W. R. Bennett, Bull. Am. Phys. Soc. 8, 87 (1963).

[14]W. R. Pendleton, Jr. and R. H. Hughes, Phys. Rev. A 138, 683 (1965).

[15]L. L. Nichols and W. E. Wilson, Appl. Opt. 7, 1697 (1968).

[16]W. Bachmann, Z. Naturforsch. A 27, 5791 (1972).

[17]W. Drtil, Z. Naturforsch. A 24, 350 (1969); 24, 1432 (1969).

[18]S. A. Kazantsev, A. Kisling, and M. P. Chaika, Opt. Spektrosk. 34, 1227 (1973) [Opt. Spectrosc. (USSR) 34, 714 (1973)].

[19]B. Buchhaupt, Z. Naturforsch. A 27, 572 (1972).

[20]C. W. T. Chien, R. E. Bardsley, and F. W. Dalby, Can. J. Phys. 50, 116 (1972).

[21]B. Descomps, J. C. Pebay-Peyroula, and J. Brossel, C. R. Acad. Sci. B 251, 941 (1960).

[22]J. P. Descoubes, in *Physics of One- and Two-Electron Atoms*, edited by F. Bopp and H. Kleinpoppen (North-Holland, Amsterdam, 1969), p. 341.

[23]A. Faure, O. Nedelec, and J. C. Pebay-Peyroula, C. R. Acad. Sci. B 256, 5088 (1963).

[24]J. Peresse, A. Pochat, and A. LeNadan, C. R. Acad. Sci. B 274, 791 (1972).

[25]I. Martinson, W. S. Bickel, J. Bromander, H. G. Berry, L. Lundin, R. Buchta, and I. Bergstrom, J. Opt. Soc. Am. 60, 352 (1970).

[26]S. A. Chin-Bing and C. E. Head, Bull. Am. Phys. Soc. 15, 1375 (1970); S. A. Chin-Bing, C. H. Head, and A. E. Greer, Am. J. Phys. 38, 352 (1970).

[27]K. A. Bridgett and T. A. King, J. Phys. B 2, 902 (1969).

[28]M. Maujean and J. P. Descoubes, C. R. Acad. Sci. B 264, 1653 (1967).

[29]R. L. Long, D. M. Cox, and S. J. Smith, J. Res. Natl. Bur. Stand. (U.S.) A 72, 521 (1968).

[30]G. A. Khayrallah, Phys. Rev. A 13, 1989 (1976).

[31]G. A. Khayrallah and S. J. Smith, Chem. Phys. Lett. 48, 289 (1977).

[32]E. A. Soa, Jenaer Jahrb. 1, 115 (1959).

[33]G. M. Lawrence (unpublished).

[34]D. M. Ryaner, A. E. McKinnon, and A. G. Szabo, Rev. Sci. Instrum. 48, 1050 (1977).

[35]P. Wahl, J. C. Auchet, and B. Donzel, Rev. Sci. Instrum. 45, 28 (1974).

[36]C. Lewis, W. R. Ware, L. J. Doemeny, and T. L. Nemzek, Rev. Sci. Instrum. 44, 107 (1973).

[37]A. Gafni, R. L. Modlin, and L. Brand, Biophys. J. 15, 263 (1975).

[38]C. A. Baker, C. J. Batty, and L. E. Williams, Nucl. Instrum. Methods 59, 125 (1968).

[39]R. E. McHose (unpublished).

[40]R. E. Imhoff and F. H. Read, Chem. Phys. Lett. 3, 652 (1969).

[41]E. Brannen, F. R. Hunt, R. H. Adlington, and R. W. Nicholls, Nature 175, 810 (1955).

[42]H. R. Moussa, Ph.D. thesis (University of Leiden, 1967) (unpublished).

[43]A. H. Mahan and A. Gallagher, Rev. Sci. Instrum. 47, 81 (1976).

[44]A. Hald, *Statistical Theory with Engineering Appli-*

cations (Wiley, New York, 1952), p. 388.
[45]D. W. Marquardt, J. Soc. Ind. Appl. Math. 11, 431 (1963).
[46]P. R. Bevington, *Data Reduction and Error Analysis for the Physical Sciences* (McGraw-Hill, New York, 1969), p. 237.
[47]Los Alamos Scientific Laboratory Report No. LA-2367 (LASL, Los Alamos, N.M.) (unpublished).
[48]R. J. Anderson, R. H. Hughes, and T. G. Norton, Phys. Rev. 181, 198 (1969).
[49]J. D. Jobe and R. M. St. John, J. Opt. Soc. Am. 57, 1449 (1967).
[50]W. Bachmann and W. Janke, Z. Naturforsch. A 28, 1821 (1973).